Eur. Phys. J. Special Topics **224**, 2755–2770 (2015)

DOI: 10.1140/epjst/e2015-02587-3

THE EUROPEAN PHYSICAL JOURNAL SPECIAL TOPICS

Regular Article

Vibration energy harvesting by a Timoshenko beam model and piezoelectric transducer

S. Stoykov[1], G. Litak[2], and E. Manoach[3]

[1] Institute of Information and Communication Technologies, Bulgarian Academy of Sciences, Acad. G. Bonchev Street, Bl. 25A, 1113 Sofia, Bulgaria
[2] Faculty of Mechanical Engineering, Lublin University of Technology, 20-618 Lublin, Poland
[3] Institute of Mechanics, Bulgarian Academy of Sciences, Acad. G. Bonchev Street, Bl. 4, 1113 Sofia, Bulgaria

Received 28 August 2015 / Received in final form 9 September 2015
Published online 20 November 2015

Abstract. An electro-mechanical system of vibrational energy harvesting is studied. The beam is excited by external and kinematic periodic forces and damped by an electrical resistor through the coupled piezoelectric transducer. Nonlinearities are introduced by stoppers limiting the transverse displacements of the beam. The interaction between the beam and the stoppers is modeled as Winkler elastic foundation. The mechanical properties of the piezoelectric layer are taken into account and the beam is modeled as a composite structure. For the examined composite beam, the geometrically nonlinear version of the Timoshenko's beam theory is assumed. The equations of motion are derived by the principle of virtual work considering large deflections. An isogeometric approach is applied for space discretization and B-Splines are used as shape functions. Finally, the power output and the efficiency of the system due to harmonic excitations are discussed. The influence of the position of the stoppers and their length on the dynamics of the beam and consequently on the power output are analyzed and presented.

1 Introduction

During the last decades the research connected with energy harvesting systems increased dramatically. The development of micro and nano technologies, smart sensors and structures, the requirements of health monitoring of different devices, defined the need of independent energy sources for small devices and self-powered sensors. A lot of devices that convert kinetic energy of structures into electrical energy have been studied theoretically and experimentally. The most popular in the engineering practice and scientific research are the devices that use piezoelectric elements as energy transducers. Among the devices which transform kinetic energy into electrical one the devices which perform nonlinear oscillations are very important [1–3].

The main advantage of nonlinear energy harvesters is that the nonlinear harvesters convert energy over a broader frequency range of vibrations. One of the simplest and mostly used mechanical systems for energy harvesting is based on a cantilever beam with tip mass [4–6]. The tip mass can interact nonlinearly via magnetic [4] or

gravitational [5] forces. The authors often accept that the mass which is connected to the tip of the cantilever is several times heavier than the beam and this allow the authors to model the beam with a tip mass as a single degree of freedom model. Such approach simplifies a lot the problem and allows studying even analytically the complex nonlinear behavior of the electromechanical system.

Broadband vibration energy harvesting based on piezoelectric converter requires nonlinear systems including mechanical resonator and piezoelectric transducer and electric circuit. In contrast to linear systems which should involve narrow band of resonance, nonlinear systems are characterized by a broader region of resonance due to the amplitude dependent resonating frequency and the existence of higher harmonics and multiple solutions.

Recently, the concept about the kinetic energy harvester model, based on nonlinear mechanical resonator and electromagnetic/piezoelectic transducers [6–8] was reviewed. Among the different types of nonlinearities those with softening and hardening are broadening the resonance regions into smaller and larger frequencies, respectively. Especially the nonlinear impacting harvesters with stoppers, derived from the idea of Soliman et al. [9] and followed in other papers [10,11]. Electrostatic and piezoelectric impacting harvesters were investigated also in [12–15].

It is important to note that the current motivation of our investigations is to combine the works of nonlinear devices forced by an excitation with composite structure of a beam. The detailed studies of piezoelectric composite beam have been performed by Erturk and Inman [3]. Most of their research was performed on linear systems and solutions were obtained by analytical methods. They also investigated nonlinear electro-mechanical couplings by using the Duffing equation for motion of the resonating beam.

In the current work, a nonlinear model for composite beams based on the geometrically nonlinear version of the Timoshenko's beam theory is used to represent the beam motion. Electro-mechanical coupling is introduced by piezo-electric constitutive equations. The contact interactions with the stoppers introduce additional nonlinearities in the equation of motion. The system of partial differential equations (PDEs) is discretized into a system of ordinary differential equations (ODEs) by the finite element method (FEM). Appropriate set of B-Splines is used for each displacement component. This formulation is preferred here because of the discontinuities in the model. They arise when the piezo layer is shorter than the main layer of the composite beam. In this case there is a jump of the thickness and the mechanical properties of the beam. Other discontinuities arise from the interaction with the stoppers. By using multiple knots, in the definition of B-Spline functions, this kind of discontinuities are modelled appropriately. The resulting system of nonlinear ODEs is solved in time domain by the Newmark's method. Newton-Raphson's method is used to solve the resulting nonlinear algebraic system. The time responses and the power output are presented in time domain for different excitation forces and base excitations, considering stoppers at different distances from the beam and assuming a tip mass on the free end.

The goal of the current work is to present more detailed and more precise theoretical and numerical model of a beam structure suitable to capture discontinuities such as jump of the thickness or impact with stoppers. Such structures are widely used in engineering applications. Particularly in the current work, several examples are presented where the beam structure is used as an energy harvester.

2 Mathematical model

The considered beam consists of two layers: a main layer which is assumed to be brass and a second layer which is from piezo material. The length of the additional

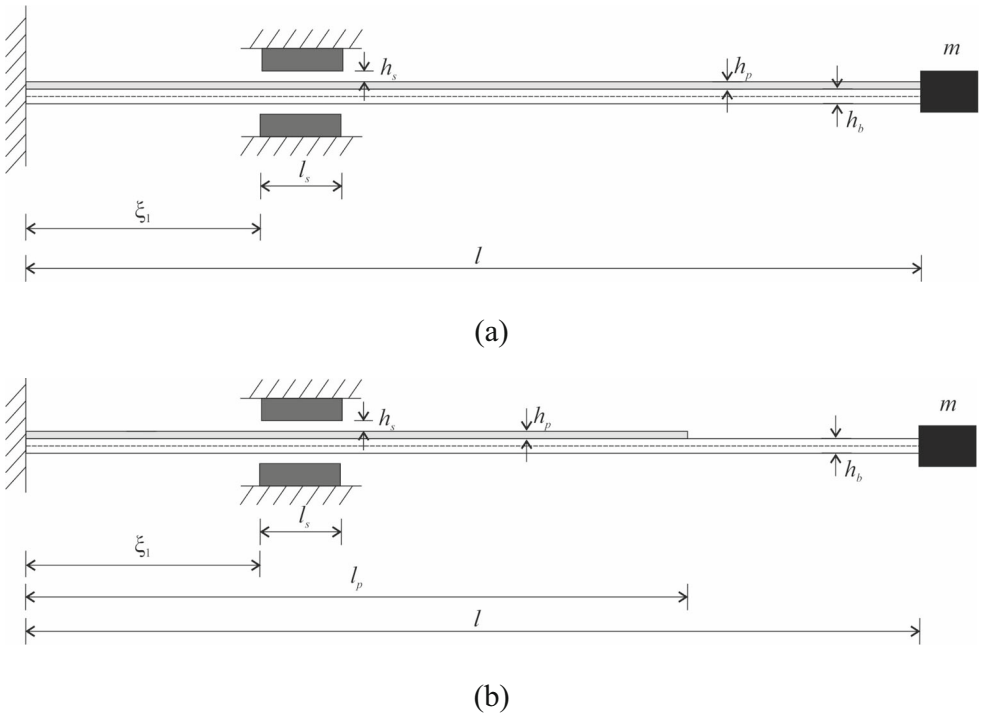

Fig. 1. Beam with stoppers and tip mass.

layer can vary. The length of the beam is denoted by l, the width is denoted by b, thickness of the layer with brass material is denoted by h_b and the thickness of the piezo layer is denoted by h_p. During its motion the beam can interact with stoppers (Fig. 1). The stoppers are positioned at distance ξ_1 from the clamped end. The length of the stoppers is denoted by l_s and the distance between the beam's surface and the stoppers is denoted by h_s. The beam carries tip mass m at its free end. It is assumed that the edge of the beam $x = 0$ is clamped to a base which can move.

2.1 Electro-mechanical coupling

The equation of motion is derived by assuming Timoshenko's theory for bending. The motion of the beam is accomplished in the horizontal plane and gravity is assumed to be negligible. The longitudinal displacement $u(x, z, t)$ and the transverse displacement $w(x, z, t)$ are expressed by the following relations [16]:

$$\begin{aligned} u(x, z, t) &= u_0(x, t) + (z - z_c)\,\phi(x, t), \\ w(x, z, t) &= w_0(x, t) + w_b(t), \end{aligned} \tag{1}$$

where $u_0(x, t)$ and $w_0(x, t)$ are the displacements of the reference line and $\phi(x, t)$ is the angle of rotation of the cross section about the axis y.

As a reference line is used the middle line of the brass layer. z_c is the position of the centroid of the cross section. $w_b(t)$ is the base excitation (the prescribed displacements of the clamped edge). It is assumed that the clamped end performs a harmonic motion. With this formulation, $w_0(x, t)$ presents the transverse displacement relative to the clamped end of the beam.

The strains are expressed by assuming Green's strain tensor [17]. Considering only the nonzero terms, the direct strain ε_x and the shear strain γ_{xz} are expressed as:

$$\begin{aligned}\varepsilon_x &= \frac{\partial u}{\partial x} + \frac{1}{2}\left(\frac{\partial w}{\partial x}\right)^2 = \frac{\partial u_0}{\partial x} + z\frac{\partial \phi}{\partial x} + \frac{1}{2}\left(\frac{\partial w_0}{\partial x}\right)^2 \\ \gamma_{xz} &= \frac{\partial w}{\partial x} + \frac{\partial u}{\partial z} = \frac{\partial w_0}{\partial x} + \phi.\end{aligned} \tag{2}$$

The piezo-electric constitutive equations are used in their reduced form [3]:

$$\begin{Bmatrix}\sigma_x \\ \tau_{xz} \\ D_3\end{Bmatrix} = \begin{bmatrix}E & 0 & -e_{31} \\ 0 & \lambda G & 0 \\ \bar{e}_{31} & 0 & \bar{\varepsilon}^s_{33}\end{bmatrix}\begin{Bmatrix}\varepsilon_x \\ \gamma_{xz} \\ E_3\end{Bmatrix}, \tag{3}$$

where σ_x and τ_{xz} are bending and shear stresses, E is the Young's modulus of the material, G is the shear modulus, λ is a shear correction factor, D_3 represents electric displacement component, $\bar{e}_{31}$ is an effective piezo-electric stress constant, $\bar{\varepsilon}^S_{33}$ is permittivity component and E_3 is electric field component. The electric field component can be presented as $E_3 = -\frac{v(t)}{h_p}$ where $v\,(t)$ is an electric potential difference (voltage) and h_p is the thickness of the piezo layer. The brass material does not have any electrical components, thus its constitutive relations are just the structural elastic components from Eq. (3).

The interaction of the beam with the stoppers is modelled as a contact interaction of the beam with a Winkler's foundation [18] with a spring constant k_w, i.e. the reaction force which arise when the moving beam reaches a stopper is:

$$R\,(x,t) = \begin{cases} k_w w_0\,(x,t) & \text{if } |w_0\,(x,t)| \geq h_s \quad \text{for} \quad \xi_1 \leq x < \xi_1 + l_s. \\ 0, & \text{otherwise} \end{cases} \tag{4}$$

The boundary conditions of the beam can be expressed as [3]:

$$\begin{aligned} u_0\,(0,t) &= 0, \\ w\,(0,t) &= w_b\,(t)\,, \\ \phi\,(0,t) &= 0, \end{aligned} \tag{5}$$

$$\begin{aligned} Ebh\frac{\partial u_0\,(x,t)}{\partial x}\bigg|_{x=l} &= -m\,\frac{\partial^2 u_0\,(x,t)}{\partial t^2}\bigg|_{x=l}, \\ \frac{\partial \phi\,(x,t)}{\partial x}\bigg|_{x=l} &= 0, \\ \lambda Gbh\left(\frac{\partial w\,(x,t)}{\partial x} + \phi\,(x,t)\right)\bigg|_{x=l} &= -\,m\left(\frac{\partial^2 w\,(l,t)}{\partial t^2}\right)\bigg|_{x=l}. \end{aligned}$$

The equation of motion is derived by the principle of virtual work:

$$\delta W_V + \delta W_{in} + \delta W_E + \delta W_{ie} + \delta W_{nc} = 0, \tag{6}$$

where δW_V is the virtual work of internal forces, δW_{in} is the virtual work of inertia forces, δW_E is the virtual work of external forces, δW_{ie} is the virtual work of internal

electrical energy and δW_{nc} is the non-conservative virtual work due to electric charge output [19]. They are given by the following expressions:

$$\begin{aligned}
\delta W_V &= -\int_V (\delta\boldsymbol{\varepsilon})^{\mathrm{T}}\boldsymbol{\sigma}\, dV,\\
\delta W_{in} &= -\int_V \rho(\delta\mathbf{d})^{\mathrm{T}}\,\ddot{\mathbf{d}} V,\\
\delta W_E &= \int_V (\delta\mathbf{d}_0)^{\mathrm{T}}\mathbf{f}_0\, dV,\\
\delta W_{ie} &= -\int_{V_p} (\delta E_3) D_3\, dV_p,\\
\delta W_{nc} &= -\delta v Q,
\end{aligned} \tag{7}$$

where $\delta\boldsymbol{\varepsilon}$ is the virtual strain vector and $\boldsymbol{\sigma}$ is the stress vector, $\delta\mathbf{d}$ is the virtual displacement vector, $\ddot{\mathbf{d}}$. represents the acceleration vector, ρ is the density, $\delta\mathbf{d}_0$ represents virtual displacements on the reference line, $\mathbf{f}_0$ is vector of external forces and moments on the reference line, δE_3 is virtual electric field component, δv is the virtual electric potential difference and Q representthe electric charge output. V represents the volume of the beam while V_p represents the volume of the piezo layer only. Integration for the virtual work of internal electrical energy is performed over the piezo layer only because there is no electrical energy for the brass layer. It is noted that the virtual works of internal and inertia forces can be separated of two integrals, for each layer, and the corresponding material properties should be used. The time derivative of electric charge output can be written as [20]:

$$\dot{Q}\frac{v}{R_1} \tag{8}$$

where R_l is the resistive load. This expression will be used in the equation of motion.

2.2 Isogeometric formulation

The discretization of the beam along its length is performed by using B-Splines. The usage of B-Splines for space discretization has advantages over the standard finite element schemes. B-Splines are used for construction of NURBS (Non-uniform rational B-Splines). NURBS can represent any conic section including circle exactly while non-rational splines or Bezier curves can only approximate it. NURBS are commonly used in computer graphics and computer-aided design (CAD). The main idea of the isogeometric analysis is to use the same basis, used to model the geometry of the object, as a basis for the solution space of the numerical method [21]. Another important feature, which is used in this work, is that by multiplying the knots, one can control the continuity of the derivatives of the basis functions. This property is very important in modelling structures with discontinuities, such as interaction with stoppers or jump of the thickness.

The definition of B-Splines and their main properties are summarized briefly below. A knot vector $\boldsymbol{\Xi} = \{\xi_1, \xi_2, \ldots, \xi_{n+p+1}\}$ is a non-decreasing set of coordinates in the parameter space, where $\xi_i \in \mathbb{R}$ is the i^{th} knot, p is the polynomial order and n is the number of basis functions. The B-Spline basis functions are defined recursively:

$$\begin{aligned}
N_{i,0}(\xi) &= \begin{cases} 1, \xi \in (\xi_i, \xi_{i+1}], \\ 0, \text{otherwise}, \end{cases} \\
N_{i,p}(\xi) &= \frac{\xi-\xi_i}{\xi_{i+p}-\xi_i} N_{i,p-1}(\xi) + \frac{\xi_{i+p+1}-\xi}{\xi_{i+p+1}-\xi_{i+1}} N_{i+1,p-1}(\xi).
\end{aligned} \tag{9}$$

If the knots are equally spaced, the knot vector is called uniform. An important property of B-Spline basis of uniform knot vector is that p^{th} order function has p-1 continuous derivatives across knots. The non-uniform knot vector gives opportunities to control smoothness and discontinuities of the derivatives of the B-Splines across the knots. If given knot ξ_i has multiplicity of m_i, then the basis functions of order p have $p - m_i$ continuous derivative across knot ξ_i. This property is important for the case of beam with layers with different lengths, which results into jump of the thickness or for modelling interaction with stoppers.

For the isogeometric formulation of the beam is necessary to define three sets of basis B-Splines for approximating the displacements $u_0(x,t)$ and $w_0(x,t)$ and the rotation $\phi(x,t)$. Let $\boldsymbol{\Xi}_u$ and $\boldsymbol{\Xi}_w$ are knot vectors that span the interval [0, 1]. The linear function

$$F(\xi) = \begin{cases} l\xi, \ \xi \in [0,1], \\ 0, \ \text{otherwise}, \end{cases} \tag{10}$$

maps one-to-one the reference interval into the interval $\Omega = [0, l]$ that represents the beam. The isogeometric basis functions on Ω, for the displacements $u_0(x,t)$ and $w_0(x,t)$ and for the rotation $\phi(x,t)$, are defined by:

$$\begin{aligned} \psi_i^u(x) &= N_{i,p_u}^u\left(F^{-1}(x)\right), \\ \psi_i^w(x) &= N_{i,p_w}^w\left(F^{-1}(x)\right) \\ \psi_i^\phi(x) &= N_{i,p_\phi}^\phi\left(F^{-1}(x)\right), \end{aligned} \tag{11}$$

and the spaces $\mathcal{V}_h^u = \text{span}\{\psi_i^u\}$, $\mathcal{V}_h^w = \text{span}\{\psi_i^w\}$ and $\mathcal{V}_h^\phi = \text{span}\left\{\psi_i^\phi\right\}$ are their isogeometric trial spaces.

The isogeometric discretization of the displacements and the rotation is expressed as:

$$\begin{aligned} u_h(x,t) &= \sum_{i=1}^{p_u} \psi_i^u(x)\, q_i^u(t) \in \mathcal{V}_h^u, \\ w_h(x,t) &= \sum_{i=1}^{p_w} \psi_i^w(x)\, q_i^w(t) \in \mathcal{V}_h^w, \\ \phi_h(x,t) &= \sum_{i=1}^{p_\phi} \psi_i^\phi(x)\, q_i^\phi(t) \in \mathcal{V}_h^\phi, \end{aligned} \tag{12}$$

where p_u, p_w and p_ϕ are the number of basis functions used for the space discretization for the displacements and the rotation. $q_i^u(t)$, $q_i^w(t)$ and $q_i^\phi(t)$ are unknown coefficients that depend on time t. They are also called vectors of generalized coordinates.

Replacing Eq. (7) into Eq. (6) and using the discretization (12), the following systems of ordinary differential equations is obtained:

$$\begin{aligned} &\mathbf{M}\ddot{\mathbf{q}} + \mathbf{C}\dot{\mathbf{q}}, + \mathbf{K_1 q} + \mathbf{K_{nl}(q)q} + \mathbf{K_w q} + \boldsymbol{\theta}_\mathbf{l} v + \boldsymbol{\theta}_\mathbf{nl}(\mathbf{q})\boldsymbol{v} = \mathbf{f}, \\ &C_p \dot{v} + Q - \boldsymbol{\theta}_\mathbf{l}^\mathbf{T}\mathbf{q} - \frac{1}{2}\boldsymbol{\theta}_\mathbf{nl}^\mathbf{T}(\mathbf{q})\,\mathbf{q} = 0. \end{aligned} \tag{13}$$

In the above equations, $\mathbf{M}$ is the mass matrix, $\mathbf{K_l}$ is the stiffness matrix of constant terms, $\mathbf{K_{nl}}(\mathbf{q})$ is the stiffness matrix that depends on the vector of generalized coordinates $\mathbf{q}$. $\mathbf{K_{nl}}(\mathbf{q})$ results from the geometrical nonlinearity of the model and introduces quadratic and cubic terms at the equation of motion, $\mathbf{C}$ is the damping matrix, $\boldsymbol{\theta}_l$ is vector of constant terms which results from the electro-mechanical coupling, $\boldsymbol{\theta}_\mathbf{nl}(\mathbf{q})$

Table 1. Geometrical and material properties of the beam layers.

	Main structure (brass)	PZT-5A
Length	0.2 m	0.2 m
Width	0.01 m	0.01 m
Thickness	0.002 m	0.001 m
Young modulus (E11)	105 GPa	60.6 GPa
Shear modulus (G)	3.9 GPa	23 GPa
Density (ρ)	9000 kg/m3	7500 kg/m3
Piezo-electric stress constant ($\bar{e_{31}}$)	-	-10.4C/m2
Permittivity constant ($\bar{\varepsilon}^{S}_{33}$)	-	13.3×10^{-9} F/m

is vector which also results from the electro-mechanical coupling but it depends linearly on the vector of generalized coordinates $\mathbf{q}$. This is also a consequence of the geometrical nonlinearity used in the model. $\mathbf{f}$ represents the vector of generalised external forces, Q represents the electric charge output on the electrodes and C_p is the corresponding capacitance.

$\mathbf{K}_w$ is matrix of constant terms which results from the interaction with the stoppers. It has the following form:

$$\mathbf{K}_w = \begin{cases} 0, & \text{if } -h_s \le w(x,t) \le h_s \quad \text{for} \quad \xi_1 \le x < \xi_1 + l_s \\ k_w \displaystyle\int_{\xi_1}^{\xi_1+l_s} \mathbf{\Psi}^{w\mathbf{T}} \mathbf{\Psi}^{w} \mathrm{d}x, & \text{otherwise.} \end{cases}$$

Taking the time derivative of the second equation from Eqs (13) and using Eq. (8), the equation of motion becomes:

$$\begin{aligned} &\mathbf{M}\ddot{\mathbf{q}} + \mathbf{C}\dot{\mathbf{q}} + \mathbf{K}_1\mathbf{q} + \mathbf{K}_{\mathbf{nl}}(\mathbf{q})\mathbf{q} + \mathbf{K}_{\boldsymbol{w}}\mathbf{q} + \boldsymbol{\theta}_1 \boldsymbol{v} + \boldsymbol{\theta}_{\mathbf{nl}}(\mathbf{q})\boldsymbol{v} = \mathbf{f}, \\ &C_p\dot{v} + \frac{v}{R_1} - \boldsymbol{\theta}_1^{\mathbf{T}}\dot{\mathbf{q}} - \boldsymbol{\theta}_{\mathbf{nl}}^{\mathbf{T}}(\mathbf{q})\dot{\mathbf{q}} = \mathbf{0}. \end{aligned} \tag{14}$$

The average power is used to compare the models and the influence of the stoppers. It is computed by the following formula:

$$P_{ave} = \frac{1}{T} \int_{t_1}^{t_1+T} \frac{v\,(t)^2}{R_l} dt, \tag{15}$$

where T is the period of vibration and t_1 is an arbitrary moment from the steady-state vibration of the beam.

3 Application

Beams composed of two layers, brass and PZT-5A, are considered for the numerical examples. The geometrical and material properties of both materials are presented in Table 1. Two types of external excitations are applied, harmonic force on the free end and kinematic excitation of the clamped edge (base excitation) according to harmonic low. Models with and without interactions with stoppers are compared and analyzed. Stoppers are positioned at different distances from the clamped end of the beam. Their length is l_s=0.005 m and the spring constant of the Winkler foundation modeling the stoppers is assumed to be $k_{\mathrm{w}} = 7 \cdot 10^6\,\mathrm{N/m^2}$. The value of the spring constant corresponds to a soft material (rubber) which is usually used to produce stoppers for engineering applications.

Table 2. Validation of the beam model with 3D FEM by comparing the natural frequencies (rad/s) of beam from Fig 1(a). The stoppers are positioned on the beam's surface for computing the natural frequencies with interaction.

Mode	Without interaction with stoppers, tip mass 0.02 g			With interaction with stoppers tip mass 0.02 g		
	Current model	Elmer 70 000 DOF	Difference %	Current model	Elmer 70 000 DOF	Difference %
1	146.57	144.98	1.10	203.72	201.47	1.12
2	1147.00	1137.90	0.80	1440.03	1430.57	0.66
3	3464.59	3438.32	0.76	3672.49	3646.86	0.70
4	7064.48	7010.48	0.77	7068.95	6989.25	1.14

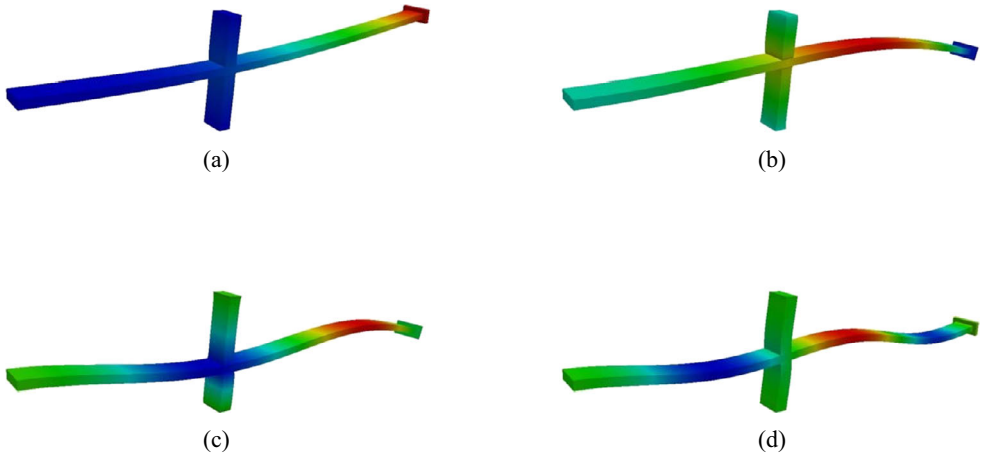

Fig. 2. Mode shapes of beam from Fig. 1(a) with tip mass of 0.02 g. The results are from 3D software. (a) First mode, (b) second mode, (c) third mode, (d) fourth mode.

3.1 Validation

The elastic part of the electro-mechanical beam model is validated by three-dimensional finite elements. Elmer software [22], which is open-source finite element software, is used to model the beam with the tip mass and the stoppers. The tip mass is modelled as elastic body with very high elastic modulus and with appropriate density in order to represent the desired mass. The stoppers are modelled as elastic bodies with Young's modulus equivalent to the one used as a spring constant which represent the Winkler foundation. The density of the stoppers is chosen to be zero in order not to influence the mass matrix, like the Winkler foundation. For the validation of the impact, the stoppers are assumed to be positioned on the beam's surface.

The comparison of the natural frequencies is summarized in Table 2 and the natural modes of the case with interaction with the stoppers are presented in Fig. 2. The validation confirms that the proposed numerical approach can be used for discontinuous problems.

3.2 Numerical results

The natural frequencies of beam presented in Fig. 1(a) but considering different weights for the tip mass are given in Table 3. The natural frequencies of beam

Table 3. Natural frequencies (rad/s) of beam (Fig. 1(a)) with and without interaction with stoppers. The stoppers are positioned on the beam's surface for computing the natural frequencies with interaction.

	Without interaction with stoppers			With interaction with stoppers		
	Without tip mass	Tip mass 0.01 kg	Tip mass 0.02 kg	Without tip mass	Tip mass 0.01 kg	Tip mass 0.02 kg
1	234.06	177.06	146.57	342.82	249.87	203.72
2	1465.40	1220.00	1147.00	1786.78	1516.14	1440.03
3	4097.02	3571.76	3464.59	4247.56	3768.05	3672.49
4	8012.60	7189.53	7064.48	8013.35	7192.72	7068.95

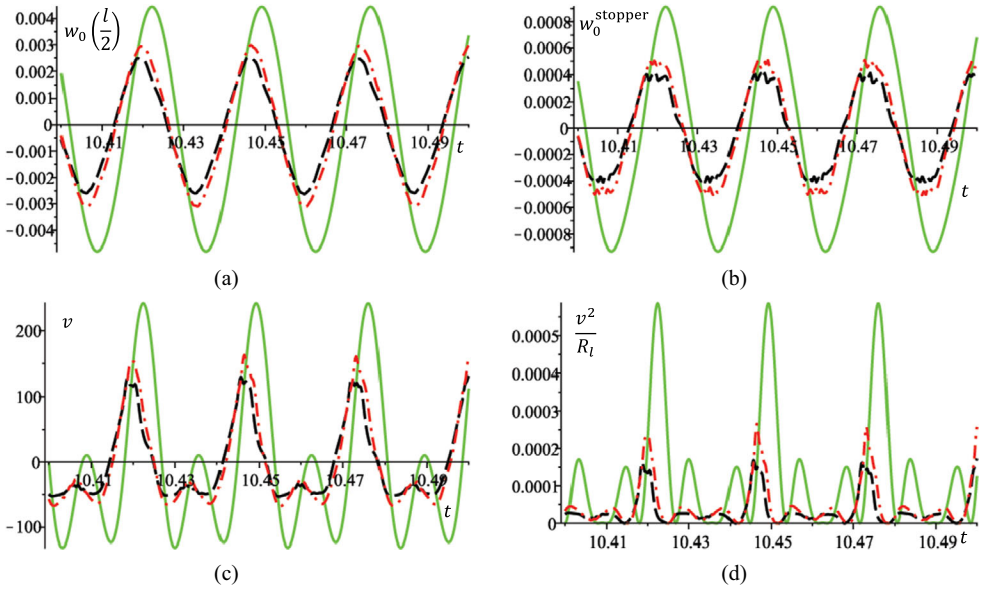

Fig. 3. Responses due to excitation force $f = 0.5\cos(234\ t)$ applied on the free end, $R_l = 10^8\Omega$. (a) Amplitude on the free end (m); (b) amplitude on the stopper (m); (c) voltage output (V); (d) power $- v^2/R_l$ (W). —— response without stoppers, $P_{ave} = 0.14$ mW, $-\cdot-\cdot-$ stoppers at distance $h_s = 0.0005$ m from the surface of the beam, $P_{ave} = 0.05$ mW, - - - - stoppers at distance $h_s = 0.0004$ m from the surface of the beam, $P_{ave} = 0.04$ mW. Piezo layer is considered to be along the whole length of the beam.

with impact are computed assuming that the stoppers are positioned directly on the surface (in the case of a contact without separation). These frequencies provide information about the resonance of the structure when the contact with the stoppers is reached. A distance between the stoppers and the beam is assumed in the numerical experiments.

First, an external force with excitation frequency equal to the fundamental frequency of the beam without tip mass and without any interaction with the stoppers is applied. Three cases are considered: without stoppers, stoppers at distances $h_s = 0.0004$ m and stoppers at distances $h_s = 0.0005$ m from the surface of the beam. The response of the beam and the output power are presented in Fig. 3.

The results demonstrate that when there are no stoppers the amplitude of vibration is bigger because the excitation frequency is equal to the fundamental natural frequency. Consequently the voltage output and the average power are also bigger. When there are stoppers, the vibration of the beam is with a smaller amplitude,

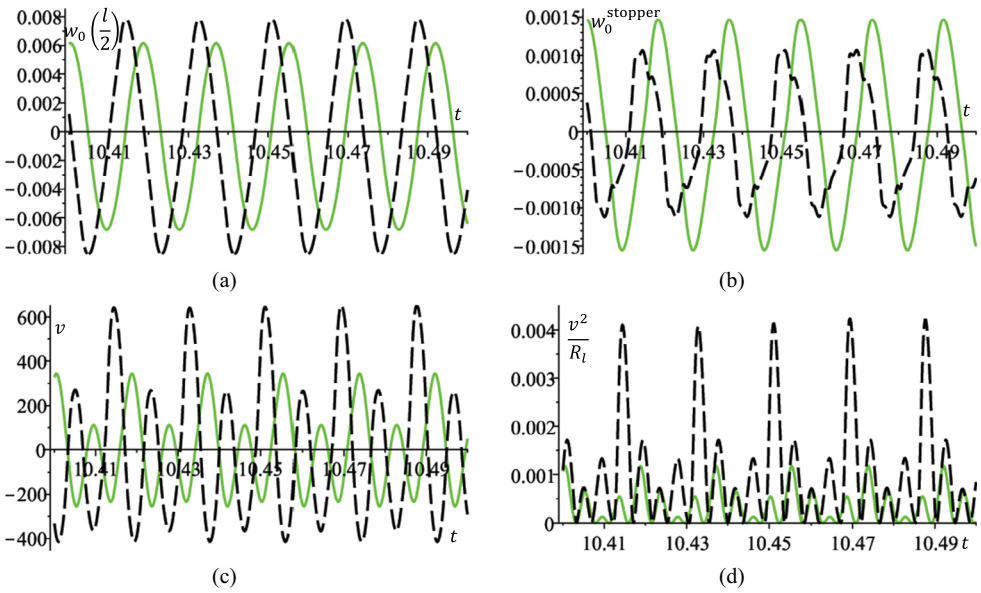

Fig. 4. Responses due to excitation force $f = 5\cos(342.8\ t)$ applied on the free end, $R_l = 10^8\Omega$. (a) Amplitude on the free end (m); (b) amplitude on the stopper (m); (c) voltage output (V); (d) power – v^2/R_l (W). —- response without stoppers, $P_{ave} = 0.33\,\text{mW}$, - - - - stoppers at distance $h_s = 0.00075\,\text{m}$ from the surface of the beam, $P_{ave} = 1.06\,\text{mW}$. Piezo layer is considered to be along the whole length of the beam.

because the excitation frequency is smaller than any natural frequency of the beam interacting with stoppers and consequently the voltage output and the power are smaller.

The numerical experiments with excitation frequency equal to the fundamental frequency of beam with interaction with stoppers are presented in Fig. 4. In this case the amplitude of vibration is larger when there are interactions with the stoppers, even though they can limit the motion. As a result, the structure generates more power.

Because of the fact that the problem is strongly nonlinear, more than one solution can exists for a given external force. Figure 5 presents two different solutions for structure with stoppers. At the first solution the beam vibrates with smaller amplitude and does not reach the stoppers, hence there is no impact. The second solution shows interaction with the stoppers and because of the fact that the excitation frequency is close to the fundamental frequency of beam interacting with the elastic foundation (stoppers), it vibrates with larger amplitude. Consequently, the power output of the case of an interaction with the stoppers is bigger. The different solutions were computed with the same configurations of external force and positions of stopper but with different initial conditions.

The following examples consider beams excited kinematically, i.e. it is assumed that the clamped end of the beam moves according to the equations:

$$w_b = a_b \cos(\omega_e t) \tag{16}$$

where a_b is the amplitude of vibration of the clamped end and ω_e is the excitation frequency.

The influence of the excitation frequency and the position of the stoppers in the generation of energy are studied. It is accepted that the stoppers are connected

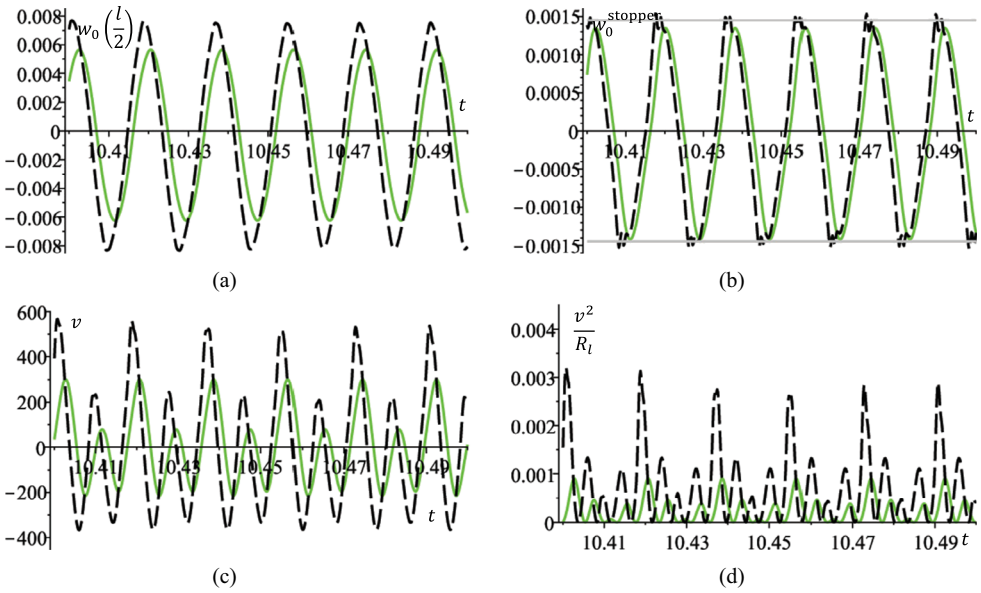

Fig. 5. Responses due to excitation force $f = 5\cos(350\,t)$ applied on the free end, $R_l = 10^8\Omega$. (a) Amplitude on the free end (m); (b) amplitude on the stopper (m); (c) voltage output (V); (d) power – v^2/R_l (W). —- periodic solution without interaction with the stoppers, $P_{ave} = 0.24\,\text{mW}$, - - - - periodic solution with interaction with the stoppers. Stoppers are at distance $h_s = 0.00145\,\text{m}$ from the surface of the beam, $P_{ave} = 0.70\,\text{mW}$. Straight grey lines on figure (b) show the position of the stoppers.

with the frame (base) at which the beam is clamped and they move according to the same law. A tip mass of 0.02 kg is considered. Model without any stoppers is compared with models with stoppers at distances $h_s = 0.0015\,\text{m}$ and $h_s = 0.002\,\text{m}$ from the beam's surface. The results are summarized in Figs 6, 7 and 8. The excitation frequency (146 rad/s) of Fig. 6 corresponds to the fundamental frequency of the beam with tip mass 0.02 kg but without any contact interaction. The excitation frequency (203 rad/s) of the graphics presented in Fig. 7 is equal to the fundamental frequency of the beam with tip mass 0.02 kg and contact interaction with stoppers (without separation). Figure 8 presents vibrations with excitation frequency (250 rad/s) bigger than the previous two and it is not close to any natural frequency.

The results from Figs. 6 and 7 differ from the observations from the previous examples. When the beam is exited kinematically, the fundamental frequency of the beam with stoppers does not lead to vibration with larger amplitude than to the one for beam without stoppers. This is shown in Fig. 7 where the frequency of the excitation ω_e is equal to the fundamental frequency of the beam with stopper. The model without stoppers vibrates with larger amplitude of vibration and consequently generates more power. Figure 8 shows that the position of the stoppers is important for efficient power generation. The excitation frequency is not close to any of the fundamental frequencies of the structure with and without impact. The model with stoppers positioned closer to the beam gives much more power than the model without stoppers. The position of the stoppers also has strong influence on the power output. The ones at distance $h_s = 0.0015\,\text{m}$ from the beam's surface generate more power output than the ones at bigger distance – 0.002 m. The average power output of the examples from Figs. 6, 7 and 8 are given in Table 4.

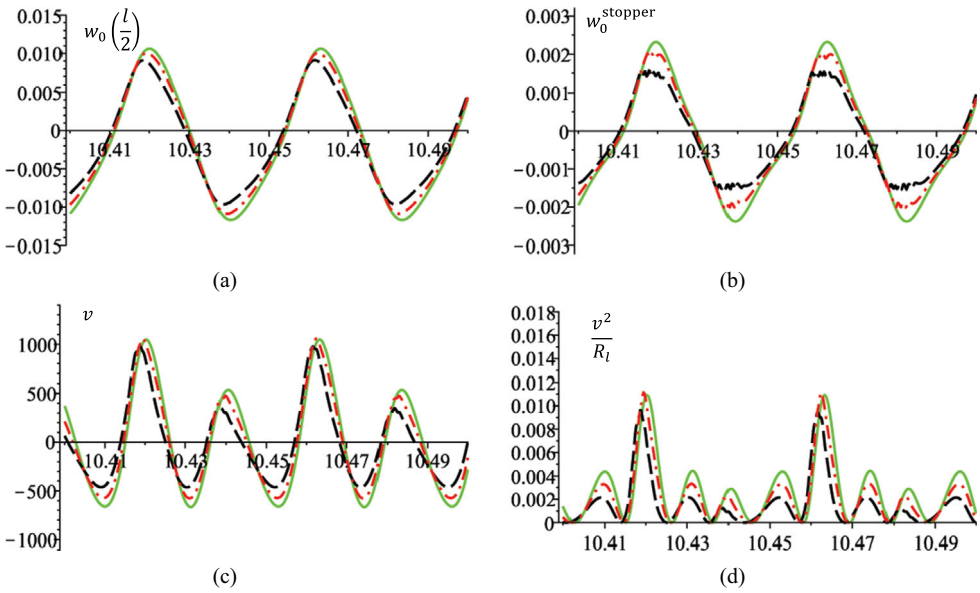

Fig. 6. Response of beam with tip mass 0.02 kg due to base excitations with amplitude 0.005 and excitation frequency 146 rad/s. $R_l = 10^8\Omega$, $k_w = 7$MPa. (a) Amplitude on the free end (m); (b) amplitude on the stopper (m); (c) voltage output (V); (d) power v^2/R_l (W). —— response without stoppers, $- \cdot - \cdot -$ stoppers at distance $h_s = 0.002$ m from the surface of the beam, stoppers at distance $h_s = 0.0015$ m from the surface of the beam.

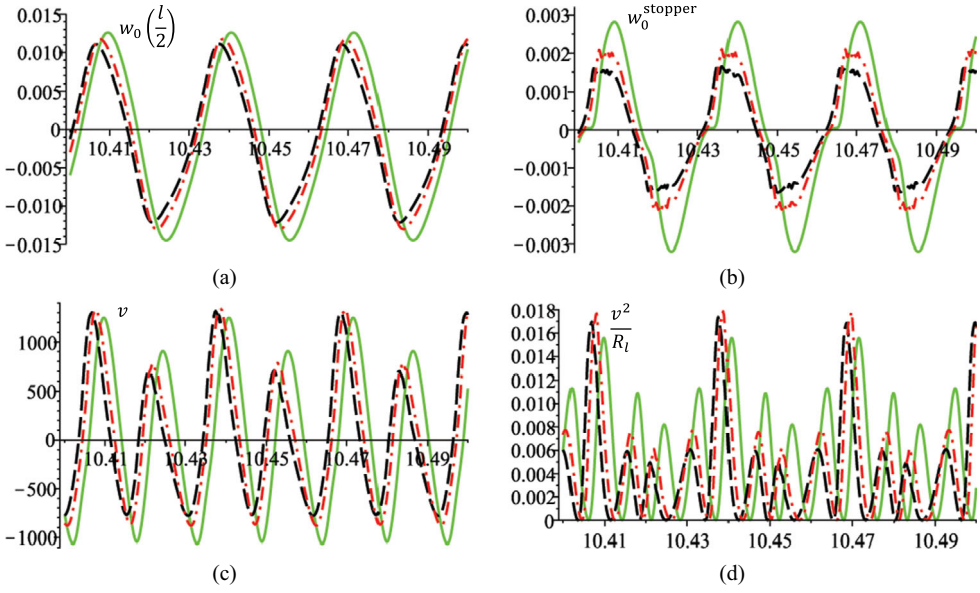

Fig. 7. Response of beam with tip mass 0.02 kg due to base excitations with amplitude 0.005 and excitation frequency 203 rad/s. $R_l = 10^8\Omega$, $k_w = 7$MPa. (a) Amplitude on the free end (m); (b) amplitude on the stopper (m); (c) voltage output (V); (d) power v^2/R_l (W). —- response without stoppers, $- \cdot - \cdot -$ stoppers at distance $h_s = 0.002$ m from the surface of the beam, - - - - stoppers at distance $h_s = 0.0015$ m from the surface of the beam.

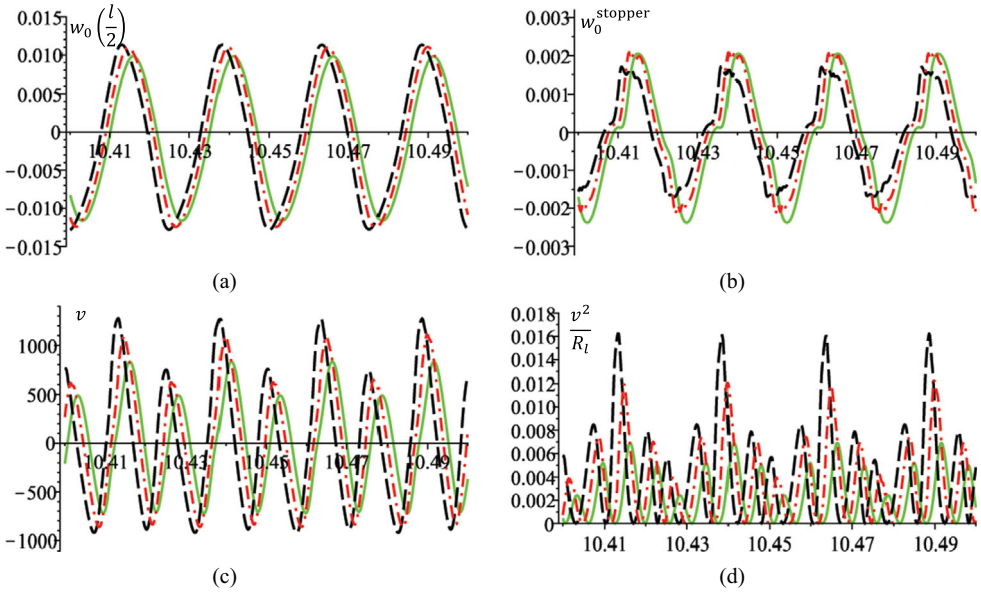

Fig. 8. Response of beam with tip mass 0.02 kg due to base excitations with amplitude 0.005 and excitation frequency 250 rad/s. $R_l = 10^8\Omega$, $k_w = 7$MPa. (a) Amplitude on the free end (m); (b) amplitude on the stopper (m); (c) voltage output (V); (d) power v^2/R_l (W). —- response without stoppers, $-\cdot-\cdot-$ stoppers at distance $h_s = 0.002$ m from the surface of the beam, - - - - stoppers at distance $h_s = 0.0015$ m from the surface of the beam.

Table 4. Average power output of examples presented in Figs. 6, 7 and 8.

$w_b = 0.005\cos(146t)$	No stoppers	2.81 mW
	$h_s = 0.002$ m	2.35 mW
	$h_s = 0.0015$ m	1.72 mW
$w_b = 0.005\cos(203t)$	No stoppers	5.42 mW
	$h_s = 0.002$ m	4.48 mW
	$h_s = 0.0015$ m	3.85 mW
$w_b = 0.005\cos(250t)$	No stoppers	2.34 mW
	$h_s = 0.002$ m	3.51 mW
	$h_s = 0.0015$ m	4.31 mW

The influence of the length of the piezo layer on the response of the system is investigated in the last numerical example. The model from the previous examples is compared with a beam structure with piezo layer equal to 3/4 from the beam's length (Fig. 1(b)). A kinematic excitation is assumed for both beams. Rigid mass on the free end is not considered. The results are computed with excitation frequency $\omega_e = 388$ rad/s. This is the fundamental frequency of the beam with length of the piezo layer equal to 3/4 of the beam's length interacting with the stoppers.

The responses of both beams without any stoppers are compared in Fig. 9. In this case, without interaction with the stoppers, the excitation frequency differs from the fundamental frequencies of both beams. The amplitudes of vibration are with almost equal amplitudes, but the voltage output and the power are different. It can be seen that the model with shorter piezo layer produces more power, i.e. the average power

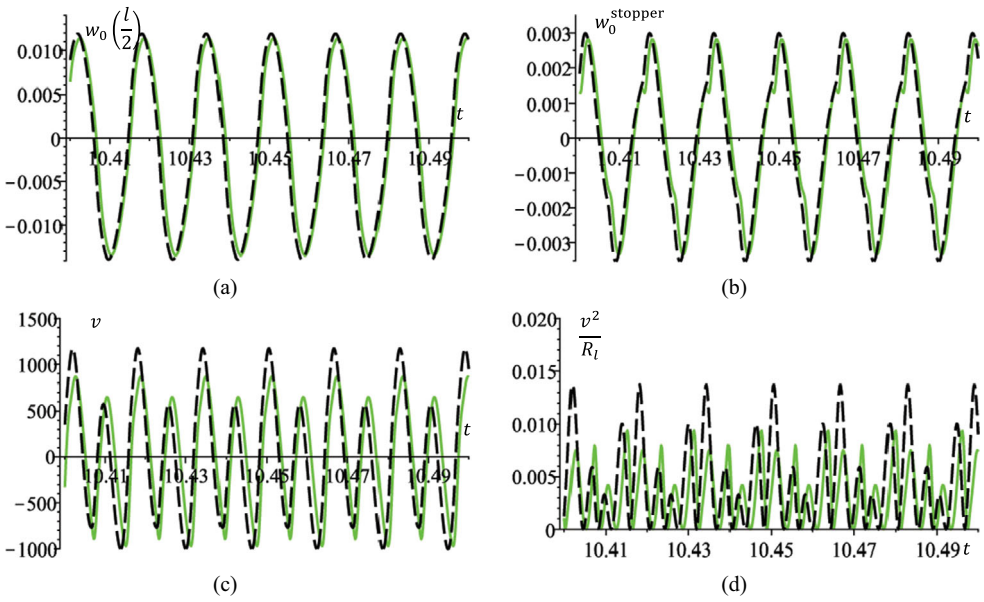

Fig. 9. Comparison of responses of beam with different length of piezo layers due to base excitations $w_b = 0.005\cos(388t)$. (——) beam with full piezo layer, $P_{ave} = 3.43\,\text{mW}$; (- - - -) beam with piezo layer equal to 3/4 of the length, $P_{ave} = 4.39\,\text{mW}$, $R_l = 10^8\Omega$, $k_w = 7$ MPa. (a) Amplitude on the free end (m); (b) amplitude on the stopper (m); (c) voltage output (V); (d) power v^2/R_l (W). Stoppers are not considered.

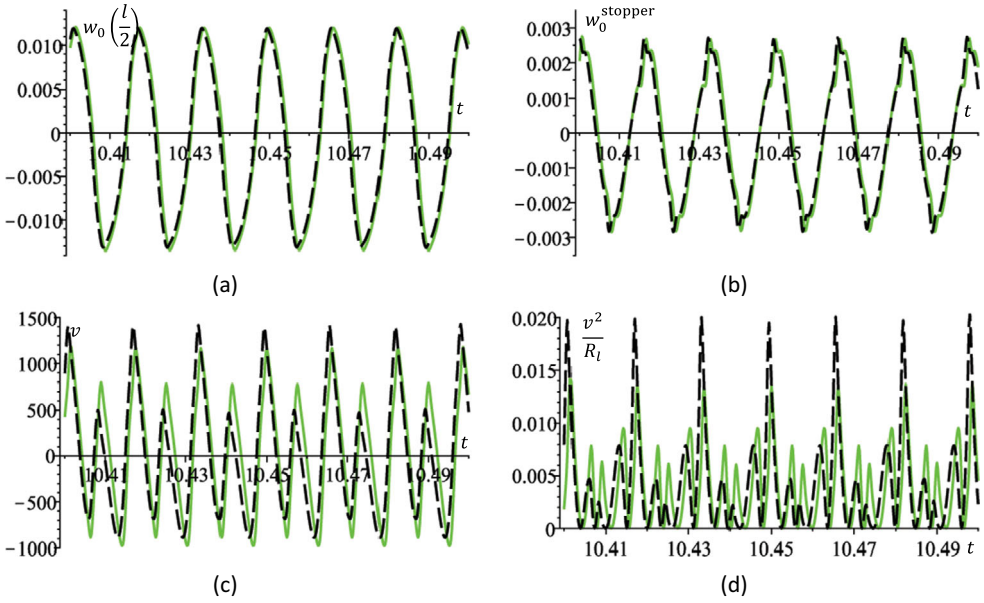

Fig. 10. Comparison of responses of beam with different length of piezo layers due to base excitations $w_b = 0.005\cos(388\ t)$. (——) beam with full piezo layer, $P_{ave} = 4.04\,\text{mW}$; (- - - -) beam with piezo layer equal to 3/4 of the length, $P_{ave} = 4.22\,\text{mW}$, $R_l = 10^8\Omega$, $k_w = 7$ MPa. (a) Amplitude on the free end (m); (b) amplitude on the stopper (m); (c) voltage output (V); (d) power v^2/R_l (W). Stoppers are positioned at distance $h_s = 0.0025\,\text{m}$.

of the model with shorter piezo layer is 4.39 mW while the average power of the model with full piezo layer is 3.43 mW.

The results of the same beams with the same kinematic excitation but with stoppers positioned at distance $h_s = 0.0025$ m are presented in Fig. 10. The average power of the model with full piezo layer increases when there is interaction with the stoppers (from 3.43 mW without stoppers to 4.04 mW). The opposite can be noticed for the beam with a shorter piezo layer, i.e. the average power decreases from 4.39 mW for the model without stoppers to 4.04 mW for the model with stoppers. This results from the limitation of the displacements of the piezo layers because of the stoppers. An important observation is the production of more power with smaller piezo layers which is valid in both cases with and without stoppers.

4 Conclusions

An electro-mechanical beam model, based on the geometrically nonlinear version of the Timoshenko's theory was developed and presented. The mechanical properties of the piezoelectric layer were taken into account and the beam was modelled as a composite structure considering large displacements. The electro-mechanical coupling was introduced into the equation of motion by piezoelectric constitutive equations. The equation of motion was derived by the principle of virtual work. The interaction of the beam with stoppers, modelled as an elastic foundation of Winkler's type, was introduced in the model. Space discretization was achieved by isogeometric approach. B-Splines with multiple knots were used for the points which introduce discontinuities in the model, like the interaction with the stoppers. An external harmonic force on the free end and kinematic excitation at the clamped end were considered.

Several numerical simulations were performed. It was shown that the stoppers can increase the power output of the system if the excitation frequency and the initial conditions are appropriate. This is related to the appearance of two solutions -resonating and non-resonating solutions, in case of stiffened characteristics of the restore force in the impacting system. Note that in contrast to a linear system where the optimization procedure is made with respect to resonance conditions, the nonlinear system is designed to work in a frequency broad band to adopt variable ambient vibration conditions.

The length of the piezo layer has influence on the response of the system. It was demonstrated that more energy can be generated with smaller piezo layer.

S. Stoykov gratefully acknowledges the support through the project AComIn "Advanced Computing for Innovation", grant 316087, funded by the FP7 Capacity Programme. G. Litak gratefully acknowledges the support of the Polish National Science Center under Grant No. 2012/05/B/ST8/00080. E. Manoach wishes to acknowledge the partial support received from the Bulgarian NSF Grant DUNK-01/3.

References

1. S.P. Beeby, M.J. Tudor, N.M. White, Meas. Sci. Technol. **17**, R175 (2006)
2. P.D. Mitcheson, E.M. Yeatman, G.K. Rao, A.S. Holmes, T.C. Green, Proc. IEEE **96**, 1457 (2008)
3. A. Erturk, D. Inman, Piezoelectric Energy Harvesting (John Wiley & Sons Ltd, Chichester, 2011)
4. F. Cottone, H. Vocca, L. Gammaitoni, Phys. Rev. Lett. **102**, 080601 (2009)

5. M.I. Friswell, S.F. Ali, O. Bilgen, S. Adhikari, A.W. Lees, G. Litak, J. Intellig. Mat. Syst. Struct. **23**, 1505 (2012)
6. S.P. Pellegrini, N. Tolu, M. Schenk, J.L. Herder, J. Intellig. Mat. Syst. Struct. **24**, 1303 (2013)
7. R.L. Harne, K.W. Wang, Smart Mat. Struct. **22**, 023001 (2013)
8. M.F. Daqaq, R. Masana, A. Erturk, D.D. Quinn, Applied Mechanics Rev. **66**, 040801 (2014)
9. M.S.M. Soliman, E.M. AbdelRahman, E.F. ElSaadany, R.R. Mansour, J. Microelectromech. Syst. **18**, 1288 (2009)
10. M. Borowiec, G. Litak, S. Lenci, Int. J. Struc. Stab. Dyn. **14**, 1440020 (2014)
11. L.-C.J. Blystad, E. Halvorsen, Microsyst. Technol. **17**, 505511 (2011)
12. L. Gu, C. Livermore, J. Smart Mater. Struct. **20**, 045004 (2011)
13. C.P. Le, E. Halvorsen, O. Sorasen, E.M. Yeatman, J. Intellig. Mat. Syst. Struct. **23**, 1409 (2012)
14. C.P. Le, E. Halvorsen, J. Micromech. Microeng. **22**, 074006 (2012)
15. K. Vijayan, M.I. Friswell, H. H. Khodaparast, S. Adhikari, Int. J. Mech. Sci. **96-97**, 101 (2015)
16. C. Wang, J. Reddy, K. Lee, Shear Deformable Beams and Plates (Elsevier, Oxford, 2000)
17. Y.C. Fung, Foundations of Solid Mechanics (Prentice-Hall, Englewood Cliffs, 1965)
18. S.Y. Lee, Y.H. Kuo, F.Y. Lin, Int. J. Sound Vib. **153**, 193 (1992)
19. A. Erturk, Comp. Struct. **106-107**, 214 (2012)
20. C.M. Junior, A. Erturk, D.J. Inman, J. Sound Vib. **327**, 9 (2009)
21. J.A. Cottrell, T.J.R. Hughes, Y. Bazilevs, Isogeometric Analysis (John Wiley & Sons Ltd, Chichester, 2009)
22. Elmer web site: `http:// www.csc.fi/elmer` (last time visited 26/08/2015)